

Tracking and Monitoring of 3-Dimensions of Welding Seam and Width in Fillet Welding of Corrugated Sheet

Yanming Quan^a and Qilin Bi^b

School of Mechanical and Automotive Engineering, South China University of Technology

Guangzhou, Guangdong 510640, China

meymquan@scut.edu.cn; bi.qilin@mail.scut.edu.cn

Correspondence Author: Qilin Bi

Abstract

To improve the traditional welding methods that cannot meet the high-quality and efficient welding requirements of the corrugated sheets and other large work pieces, a visible and intelligent method to monitor the fillet welding of corrugated sheets and the equipment were researched. A system based on single laser line to track the assembly gap to be welded was developed and built. First, a system consisting of work-piece, torch, laser, and camera was assembled to monitor the fillet welding, and the coordinates for the motion platform, camera, and image were established. Then, according to the image of projection lines, a model was developed to analyze and calculate the change in width and position of the assembly gap caused by the undulating edge and deformation of the corrugated sheet and base plate. Finally, the work-piece was measured by contacting method and the result was compared with that obtained by automatic monitoring based on the visual sensors. The results indicated that the monitoring of width and trajectory of the assembly gap can reach an accuracy of $\pm 0.5\text{mm}$. This level of precision is sufficient for the requirements of controlling the torch and adjusting welding parameters in automatic welding of container corrugated sheet.

Keywords: *corrugated sheet; automatic welding; visual tracking; assembly gap; 3-dimensional trajectory*

1. Introduction

Welding seam tracking and monitoring (WSTM) is one of the key underlying technologies in automated welding techniques and equipment. The assembly gap being welded (AG-W) is the object for tracking and monitoring in the welding process. With increasing volume of products from modern industrial manufacturing, a large number of parts are assembled by welding. Thus the welding quality, efficiency, accuracy, etc., are dependent on WSTM. The traditional control methods of WSTM are eye recognition, mechanical cam, electromagnetic sensor, ultrasonic sensor and similar techniques. Wu *et al.* [1] studied the arc sensors and S. Chokkalingham *et al.* [2] investigated on visual sensors. These methods and apparatus are used in specific applications.

The method of tracking and monitoring welding seam based on laser to analyze AG-W, uses the image of laser line modulated by the gap of work-piece assembly. This method has high-speed, and is precise and real-time. It is widely applied in welding seam tracking monitoring worldwide for the past two decades. For example, for a flat butt welding with groove, Yu *et al.* [3] collected the triangular image of the laser projection line modulated by the groove being welded to obtain 3-dimensional information of the welding seam. The flat butt automatic welding of titanium alloys was researched by Luo and Chen [4] based on the similar principles.

To reduce the advance errors caused by the single line laser, a scanning sensing system based on two line laser is proposed by Kim *et al.* [5]. The AG-W is irradiated by two line laser at a predetermined angle. The two laser projection lines are parallel to each other and perpendicular to the AG-W and the camera is vertical to the work platform. Qiao *et al.* [6] simplified the structure on this basis, using a beam splitting lens to separate the light to obtain two laser projection lines parallel to each other. Wu *et al.* [7] studied a scanning system in which a dot laser rotates around a centerline and a camera fixed on this line captures the images. Xu *et al.* [8] made some structural improvements to this system. A lens is rotated in front of a fixed line laser, and a round spot is acquired. Lu [9] assembled a circular weld inspection system based on laser scanning vision sensor. Huang *et al.* [10] calculated the trajectory of 3-dimensional welding seam and the width of seam gap using the following system and strategy. The two lasers are arranged in bilateral symmetry of the camera to project two red parallel lines, and two lasers are arranged anteriorly and posteriorly of the camera to project two green parallel lines. Moreover, all the structured light lines are parallel to each other. The spatial coordinates of projection plane is calculated according the red laser projection lines and the two-dimensional trajectory of welding seam on the projection plane and the width of seam gap are calculated according to the green laser projection lines.

The research efforts described above are mainly related to flat butt welding. Generally, the welding seams are recognized according to laser line projection modulated by the geometric structure of large groove. Few studies involve narrow butt welding, and the studies on fillet welding, especially corrugated plate welding are scarce. For fillet welding of large structures, space to accommodate large monitoring devices is limited, and also there is no groove to modulate the laser line. Thus, it is more difficult to monitor the fillet welding than the flat butt welding with groove. The low strength, large deformation, errors in machining and assembly, and cycled crease of seam, cause the real AG-W seam trajectory to deviate from the planned trajectory randomly and significantly. The thermal deformation during the welding process changes the AG-W further. To ensure welding quality, the welding controller needs to dynamically measure the width of assembly gap and center position to adjust the welding parameters and welding trajectory. However, WSTM equipment based on such principles is not easily available. There are only a few patents of trajectory tracking devices based on laser ranging. Tian *et al.* [11] assumed that the base plate to be welded is an ideal level plane in the automatic welding of the corrugated sheet of container. The laser spot is projected on the corrugated sheet and base plate. The trajectory of the seamless contacting curve between the corrugated sheet and base plate is obtained from the feedback signal of laser spot. In fact, as the difference in heights between the edge of corrugated sheet and base plate is about 10mm in the direction of length of 10m, it is difficult to monitor the width of AG-W with this method. A method of using two visual devices to identify the pool image and laser line projection respectively for tracking and monitoring the fillet weld of corrugated sheet was proposed by the authors of this paper, Bi and Quan [12]. But the calculations and analysis are also based on the assumption that the plate to be welded is a level plane, which introduces some errors in actual applications. Meta Vision Systems [13] could recognize the 3D trajectory of assemble gap in many cases, but in the fillet welding of corrugation tracking processing, if the camera not rotate with the axis of the torch, the object distance will change in the part of plotline and the imaging was fuzzy; if the camera rotate with the axis of the torch, the camera will be intervene with the corrugated sheet.

In this paper, the undulating corrugated sheet edge and base plate surface and the deformation of the corrugated sheet are taken into consideration, and a model to analyze and calculate the changes in seam width and the trajectory is proposed. An

experiment was designed to verify accuracy of the proposed model. This method is capable of tracking and monitoring the 3D trajectory and gap width of fillet welding of corrugation online in high speed MAG welding processing

2. Tracking and Monitoring System

Figure 1 shows the system to track and monitor the fillet welding of corrugated sheet based on single line laser. It consists of the torch, laser line generators, industrial camera, working platform, welding parameter adjuster, motion controller and few other components.

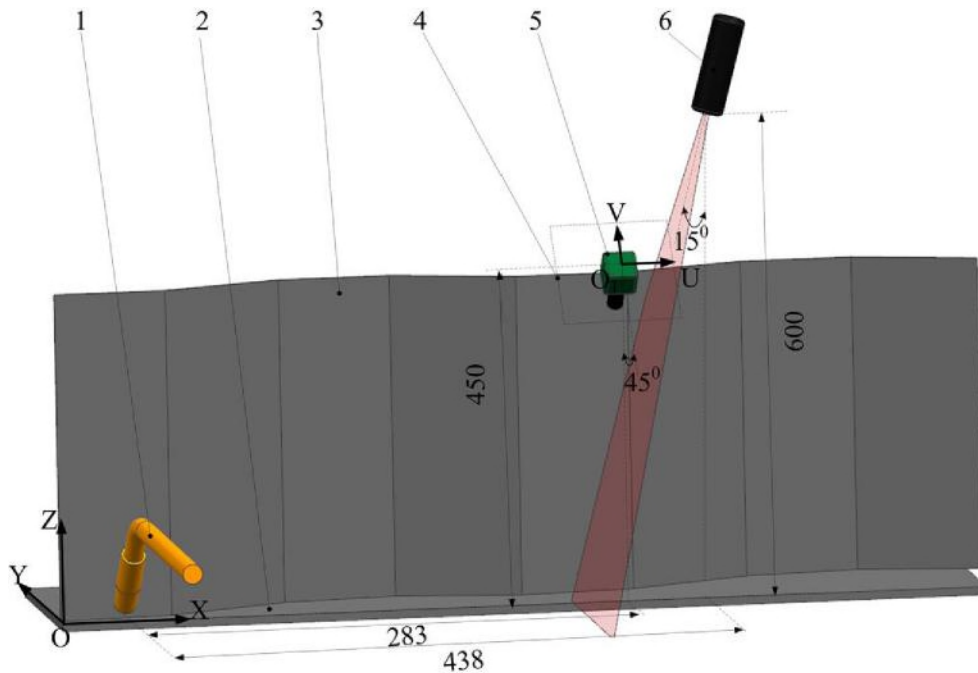


Figure 1. The Schematic Diagram Showing the Installation and Operation of Tracking and Monitoring System: 1. The Torch, 2. The Base Plate, 3. The Corrugated Sheet, 4. The Imaging Surface, 5. The Camera, 6. The Laser

The origin (O) of global coordinate system XYZ is the starting point of welding process. The directions of x-axis and z-axis are along the length of the table and height of the corrugated sheet respectively. The direction of y-axis is along the normal to xz plane. To prevent the laser line projection from being blocked by the corrugated sheet, the axis of laser line is made to form an angle of 15° with z-axis in xz plane, and the luminous point of laser line is adjusted so that it is 600mm from xy plane, 200mm from xz plane, and 438mm from the torch along the x-axis. The laser line projected on the base plate is perpendicular to the x-axis. The center point O1 of the imaging plane of camera is 450mm from the xy-plane, 450mm from the xz-plane, and 283mm from the torch along x-axis. An angle of 45° between the axis of camera and z-axis in the xy-plane is maintained to facilitate capture of the laser line projected on the corrugated sheet and base plate, and to prevent any interference between the camera and corrugated sheet. The imaging surface is parallel to the x-axis. For convenience, it is assumed that the plane in which image is displayed is parallel to the imaging plane of the camera. In the welding process, the lasers, camera and the torch translate along the trajectory of the corrugated sheet, and do not rotate while moving along slope of the corrugated sheet. If there is

no seam between the corrugated sheet and base plate because of close contact, the laser lines projected on them will intersect at the point M, the coordinates of which in the image plane uv are (U_M, V_M) , as shown in Figure 2-a. If there is a seam between the corrugated sheet and base plate because of no contact, the laser line projected on them will have two endpoints M and N, the coordinates of which in the image plane UV are (U_M, V_M) and (U_N, V_N) respectively, as shown in Figures 2-b and 2-c. Employing the coordinates of the endpoints of the laser projection lines images, the image processing technology, and model for calculating calculations and analysis, the position of the camera in the coordinates system XYZ , the real width of the welding seam and the trajectory of the centerline of the AG-W are established, and the dynamic monitoring is achieved.

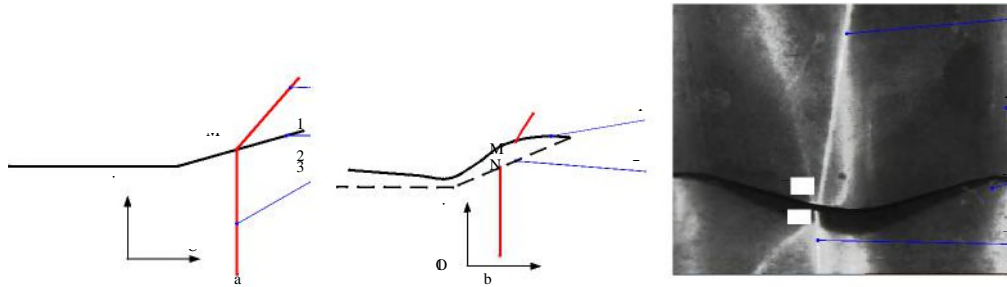


Figure 2. The Laser Projection Line: (a) AG-W without Gap: 1. The Laser Line Projected on the Corrugated Sheet, 2. The Edge of the Corrugated Sheet, 3. The Laser Line Projected on the Base Plate, (b) The Existing Gap in AG-W: 1. The Actual Edge of the Corrugated Sheet, 2. The Theoretical Edge of the Corrugated Sheet, (c) The Laser Projection Line with Gap: 1. The Laser Line Projected on the Corrugated Sheet, 2. The Corrugated Sheet, 3. The Base Plate, 4. The Laser Line Projected on the Base Plate

01

3. The Actual Gap width of AG-W

The actual width S is defined as the distance between a boundary edge of the corrugated sheet and the centerline of the base plate. The coordinates in the imaging plane are (U_M, V_M) , (U_N, V_N) respectively.

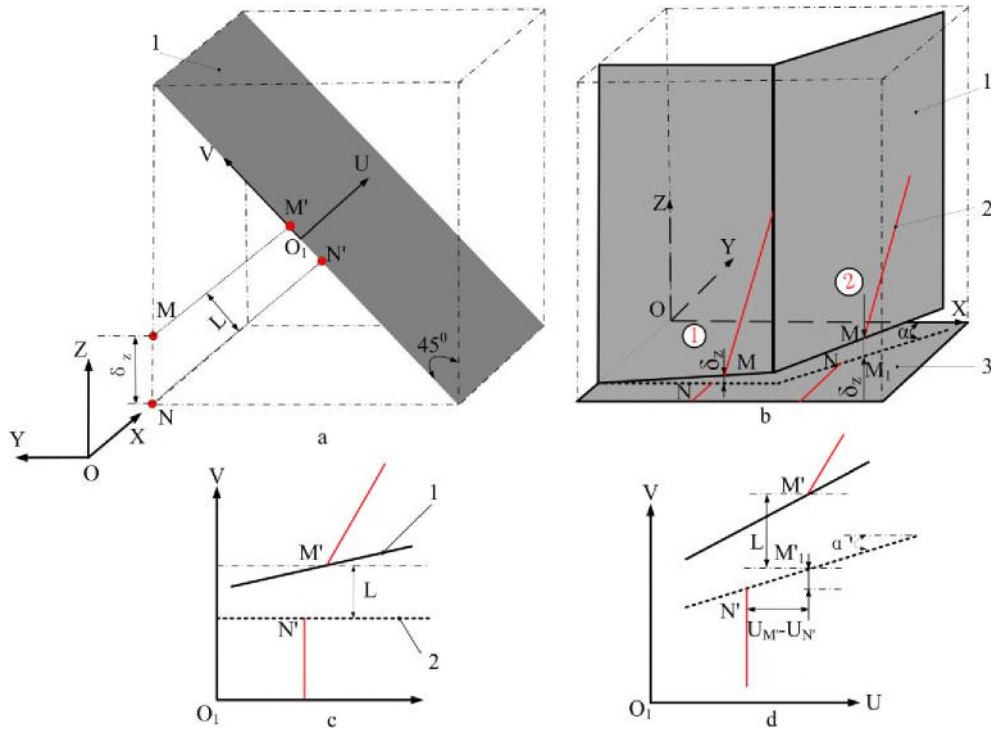


Figure 3. The Principles of Actual Seam Width Evaluation: (a) The Relationship between the UV Imaging Plane and XYZ Coordinate System,; 1. The UV Imaging Plane, (b) The Laser Projection Line: 1. The Corrugated Sheet, 2. The Laser Projection Line, 3. The Base Plate, (c) The Image of the Laser Projection Line in Stage ①: 1. The Image of Actual Edge of the Corrugated Sheet, 2. The Projected Edge of the Corrugated Sheet on the Base Plate along the z-axis, (d) Image of the Laser Projection Line in Stage ②

3.1 The Projected Line on Stages ① and ③

According to the definition, the width of AG-W is δz , is shown in Figures 3-a, and 3-b, and it corresponds to the image L in the UVW coordinate system, as shown in Figure 3-c.

According to the coordinates of endpoint endpoints M and N of the laser projection line in UV imaging plane, (as shown in Figure 3-c), L should satisfy the following relationship:

$$L = \frac{v_M - v_N}{u_M - u_N} \quad (1)$$

According to the spatial position of the uv imaging plane of the camera in coordinate system XYZ (as shown in Figure 3-a) and the calibration value ζ in the uv imaging plane, the actual value δz of the width of AG-W can be determined from the following relationship:

$$(2)$$

ã

3.2 The Projected Line on Stages ② and ④

In this stage, the angle between the projection of the edge of the corrugated plate on the xy plane and the x -axis is α . The point M_1 is the projection of point M on base plane along the z -axis and the image of it is M'_1 in the uv imaging plane, as shown in Figure 3-b. In this case, the distance between the points M' and M'_1 and L

which is width of the image of the gap width δ_z of AG-W should satisfy the following relationships:

$$(3)$$

The angle α in xy plane is projected on the uv plane. The angle α' is the projected angle of α . On the basis of the spatial relationship between uv plane and xy plane, the following relationship is obtained.

$$(4)$$

By simplifying the equations (3) and (4), and combining the result with the relationship between the actual seam width δ_z and image width L of the weld seam (given by equation (2)), the value δ_z of the actual seam width of AG-W as shown by equation (5) can be obtained.

$$(5)$$

4. The Actual Trajectory of AG-W

The theoretical trajectory is defined as the centerline of theoretical gap between the corrugated sheet and base plate to be welded. The theoretical assembly gap is obtained from the designed dimensions of the work-pieces and the geometrical relationship of their assembly. In the Computer Numerical Control (CNC) machine controlled welding process, the line laser and camera move together along the theoretical trajectory of the centerline of AG-W at a constant velocity in the direction of x-axis. The theoretical trajectory of centerline of AG-W is shown as a broken line 2 in Figure 4-a. In fact, the corrugated sheet is deformed in the process of cutting and assembly, and causes error in assembly along the y-axis. It is shown as a broken line 1 in Figure 4-a. The photograph of assembly gap is shown in Figure 4-b.

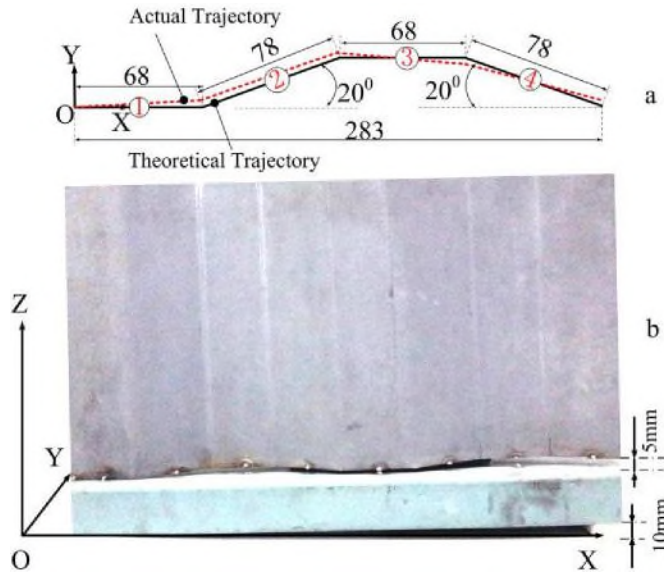


Figure 4. The Trajectory of Centerline of the AG-W: (a) The Trajectory of Centerline of the AG-W in XY Plane: 1. The Actual Trajectory, 2. The Theoretical Trajectory, (b) The Photograph of the Assembly Gap

4.1 The Y-coordinate of Actual Trajectory

It is assumed that the theoretical trajectory of AG-W between the corrugated sheet and base plate passes through point $C_0(x_{C0}, y_{C0}, z_{C0})$ for a moment. The geometrical analysis is completed on the yz and uv imaging planes, shown in Figure 5. The corresponding point of C_0 in the uv imaging plane is the point $C'_0(u_{C'0}, v_{C'0})$. In this case, if the trajectory of the actual AG-W deviates from the theoretical AG-W in XY plane, for example: the endpoints of the laser lines projected on the corrugated sheet and base plane are $M(x_M, y_M, z_M)$, $N(x_N, y_N, z_N)$ respectively, and their center point is the point $C(x_C, y_C, z_C)$ and the corresponding points of C , M , and N in the uv imaging plane are the points $C'(u_{C'}, v_{C'})$, $M'(u_{M'}, v_{M'})$, $N'(u_{N'}, v_{N'})$ respectively. Therefore the amount of offset is $y_C - y_{C0}$ along y-axis. The coordinate y_{C0} is the y-coordinate of a point on the theoretical trajectory and is known, and, y_C can be obtained through image analysis.

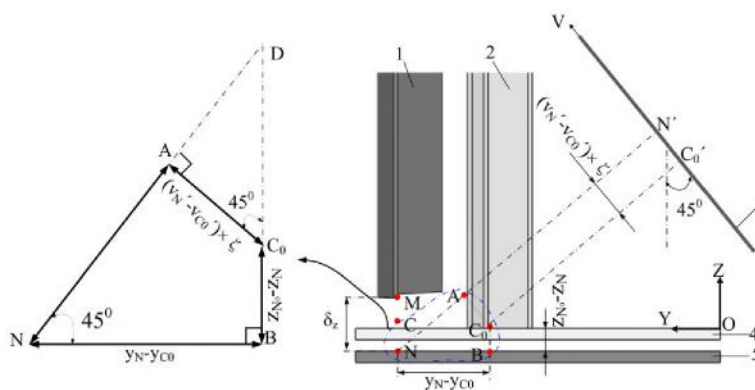


Figure 5. The Principle of Acquiring the Actual Trajectory of Centerline of AG-W along y-axis: 1. The Actual Position of the Corrugated Sheet, 2. The Theoretical Position of the Corrugated Sheet, 3. The UV Imaging Plane, 4. The Theoretical Position of the Base Plate, 5. The Actual Position of the Base Plate

In Figure 5, the point of C_0 projected on the theoretical base plate along z-axis is point B; AC_0 is the distance between the points N and B along the v-axis in the uv imaging plane; the point D is the intersection of the lines BC_0 and NA . According to the coordinates of image of laser line projection, the position of camera in XYZ coordinate system and the calibration value ζ (mm / pixel) in imaging plane uv, the following relationships can be obtained.

$$\begin{aligned}
 AC_0 &= v_c - v_n \\
 &= (N' - c) \\
 \frac{NB}{y_c - y_n} &= \frac{NC_0}{y_c - y_n} \\
 \frac{y_c - y_n}{y_c - y_n} &= \frac{cN}{cN}
 \end{aligned} \tag{6}$$

In the YZ plane, the following relationships can be obtained from the plane geometry relationships.

$$\tag{7}$$

On substituting the equations (6) in equations (7) and simplification the Y-coordinate of the point C can be obtained as shown by equation (8).

$$\tag{8}$$

BC_0 is the offset between the actual and theoretical positions of base plate. The equation (4) is substituted in equation (8) and the equations (9) are obtained.

$$\begin{aligned}
 & \text{---} \tag{9} \\
 & \frac{2}{\sqrt{3}} (v_n - v_c) \times \\
 & \frac{1}{\sqrt{3}} 2(v_n - v_c) \times \\
 & \text{---} \\
 & \text{---} \tag{10} \\
 & 2 \times \left[2(v_n - v_c) \tan(\arctan \frac{u_n - u_n'}{v_n - v_c}) \right] < C \text{ stages } \text{---} \text{ and}
 \end{aligned}$$

4.2 The Z-coordinate of Actual Trajectory

When the actual position of the base plate to be welded is above or below the theoretical position, there is an offset between the position of end point N' of the laser line projected on base plate in the uv imaging plane and the point C'_0 on the right or left of u -axis, as shown in Figure 6.

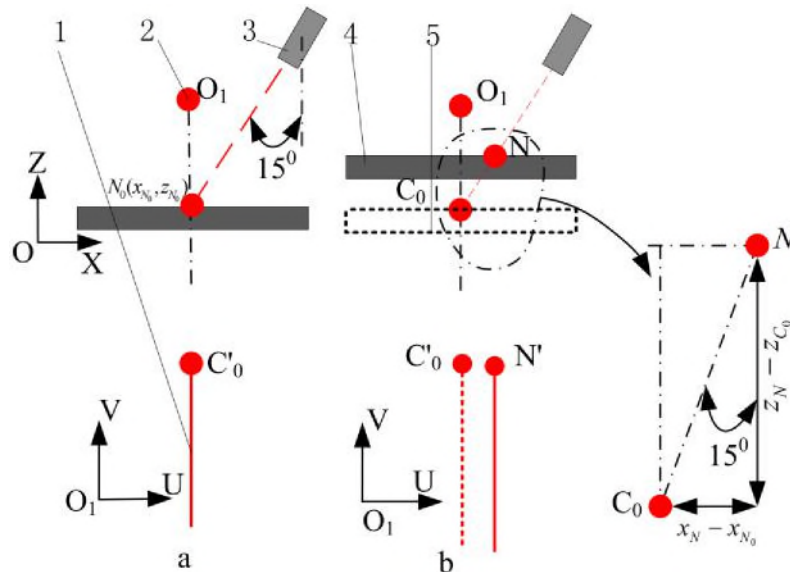


Figure 6. The Principle of Acquiring the Actual Trajectory of the Centerline of AG-W along z-axis: (a) The Base Plate at the Theoretical Position: 1. The Laser Projection Line, 2. The Center Point of uv Imaging Plane, 3. The Laser, 4. The Actual Position of the Base Plate, 5. The Theoretical Position of the Base Plate, (b) The Base Plate at Actual Position

\bar{x}

$N \quad \sigma$

\bar{z}

σ

The coordinates of images of laser projection lines' endpoints, the calibration value ζ (mm / pixel) in uv imaging plane, the image offset along u-axis and the image offset along x-axis should satisfy the following relationship.

$$\left(\begin{matrix} u \\ v \end{matrix} \right) = \zeta \left(\begin{matrix} x_N - x_{N_0} \\ z_N - z_{C_0} \end{matrix} \right)$$

\bar{z}

\bar{z}

(10) From the positions of the laser generator and the camera in the coordinate system XYZ, the actual value z_N of the base plate to be welded along z-axis is deduced. z_N should

satisfy the following relationship:

$$\frac{N}{\dots} = \dots \quad (11)$$

Therefore, the z-coordinate of upper surface of the base plate to be welded should satisfy the following relationship.

t a n l 5

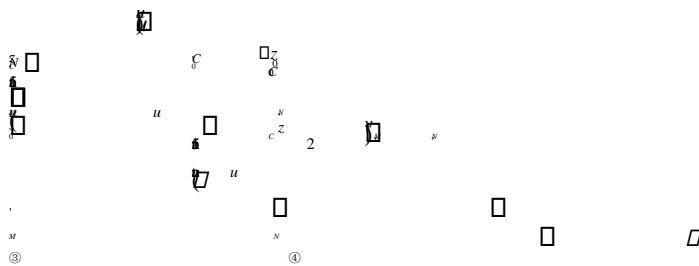
The comprehensive analysis of the value Z_c of the actual centerline of AG₁W along the z-axis shows that it is composed of the value Z_N of the point N projected on upper surface of actual base plate to be welded along the z-axis and the seam width b_z , and that it should satisfy the following relationship.

$$Z_c = Z_N + \frac{b_z}{2} \quad (13)$$

(10)

From the equations (2), (5), (12), and (13), the z-coordinate of point C on the actual trajectory of centerline of AG-W of stages ① and ③ and stages ② and ④ is obtained.

$$(14)$$



5. Experiments and Analysis of the Results

Figure 4-3 shows the experimental setup for the AG-W process. The setup includes a base plate, a corrugated sheet, and a laser module. The laser module is used to track the trajectory of the centerline of the AG-W process. The setup is shown in a perspective view, with the z-axis pointing upwards and the x and y axes forming a horizontal plane.

Figure 4-4 shows the experimental setup for the AG-W process. The setup includes a base plate, a corrugated sheet, and a laser module. The laser module is used to track the trajectory of the centerline of the AG-W process. The setup is shown in a perspective view, with the z-axis pointing upwards and the x and y axes forming a horizontal plane.

Figure 4-5 shows the experimental setup for the AG-W process. The setup includes a base plate, a corrugated sheet, and a laser module. The laser module is used to track the trajectory of the centerline of the AG-W process. The setup is shown in a perspective view, with the z-axis pointing upwards and the x and y axes forming a horizontal plane.

Figure 4-6 shows the experimental setup for the AG-W process. The setup includes a base plate, a corrugated sheet, and a laser module. The laser module is used to track the trajectory of the centerline of the AG-W process. The setup is shown in a perspective view, with the z-axis pointing upwards and the x and y axes forming a horizontal plane.

Figure 4-7 shows the experimental setup for the AG-W process. The setup includes a base plate, a corrugated sheet, and a laser module. The laser module is used to track the trajectory of the centerline of the AG-W process. The setup is shown in a perspective view, with the z-axis pointing upwards and the x and y axes forming a horizontal plane.

5.1 The Experimental Conditions

The work-piece of the experiment was a part of container's corrugated sheet (two corrugate cycles' length), and the thickness of the corrugated sheet was 2mm. The theoretical size of a single cycle is shown in Figure 4-1. To verify that the proposed method can track and monitor the change in seam width of AG-W, the corrugated sheet and the base plate were assembled initially by spot welding, before they were joined by continuous welding. The seam width at starting point of AG-W was 0mm and increased to 5mm at the point of finish. A seam of gradually increasing width between the base plate and the corrugated sheet was obtained. Also, to verify that the proposed method can track and monitor the changes in the trajectory of AG-W, the finishing side of bottom surface of base plate was positioned 10 mm above than the starting side. The physical arrangement of the work-piece is shown in Figure 4-5. The two-dimensional motion platform moves along the trajectory of the rippe seam, with the work-piece fixed on it. The LabVIEW 2010 software was used for programming. The domestic monochrome digital camera (2,000,000pixels), computer lens (f=25

were used in the experiment. In the experimental process, the camera and laser line generator are stationary. To calibrate the camera parameters and reduce distortion error, the projector calibration method and first-order radial distortion model were adopted by Xie and Quan [14]. The internal parameters of camera were computed, and the results are shown in table 1.

Table 1. The Internal Parameters of the Camera and Projector

Name	The coordinate of point u-axis	The coordinate of point v-axis	The scale factor of u-axis	The scale factor of v-axis	The parameter of first-order radial distortion k1
Camera	526.70	324.93	3185.22	3194.12	-0.12
Projector	995.54	350.80	2174.34	2158.18	0.02

5.2 The Image Acquisition and Processing

During the tests, the light reflected from metal surface was found to be interfering seriously in obtaining the image of the laser projection line. When the camera aperture parameter was inappropriate, the quality of image was found very poor, as shown in Figure 2-c. After comparing the results from many experiments,



an aperture parameter $f/1.4$ was determined as the best. With this aperture the imaging of laser projection line was clear, the characteristics of the image were more obvious, and the interference was less serious. Under control of the program, the two-dimensional platform was made to move along x-axis at a speed of 0.3m/min, 0.6m/min, and 1.2m/min. Through tests, the focal length of visual system, aperture and other parameters were optimized for obtaining best results. Before beginning continuous welding, the frame frequency was set at 50frames/s and the laser lines projected on the corrugated sheet and base plate were captured, as shown in Figure 7.

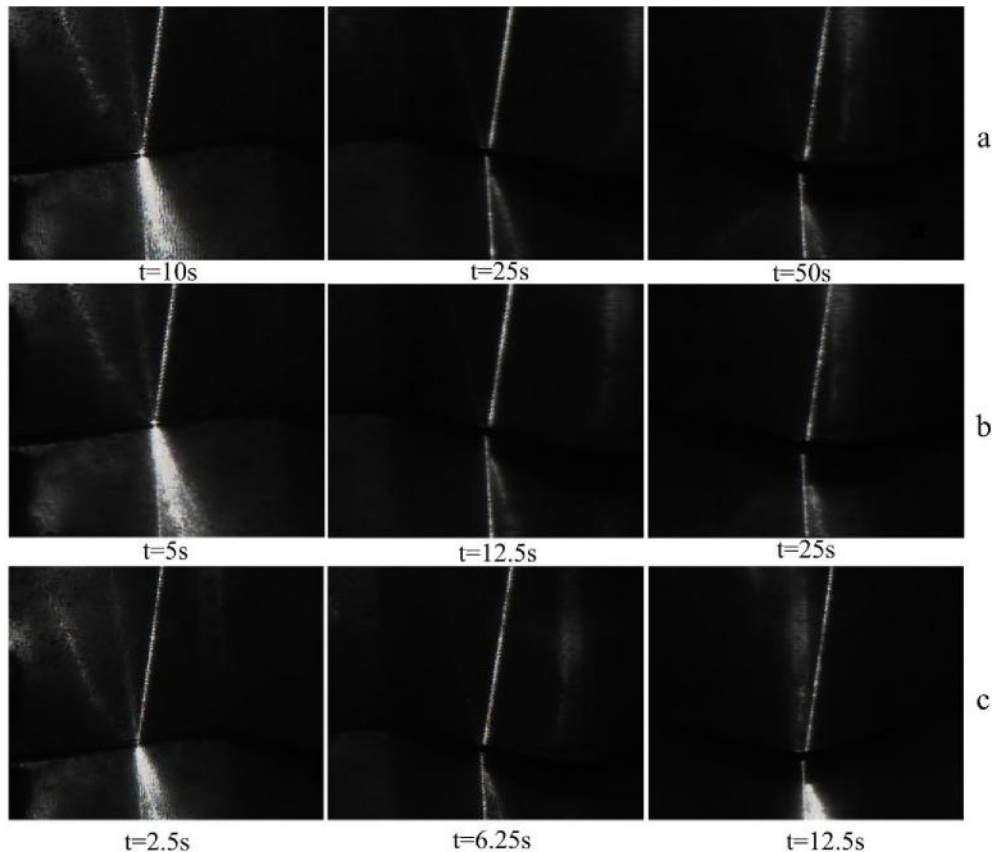


Figure 7. The Laser Lines Projected on the Corrugated Sheet and Base Plate: (a) The Platform Moving Along x-axis at a Speed of 0.3m/min, (b) The Platform Moving along x-axis at a Speed of 0.6m/min, (c) The Platform Moving along x-axis at a Speed of 1.2m/min

The arc interference does not appear in the images because of the distance of 283mm, a cover plate between arc and the field of view of the camera, and adoption of a small aperture. The image features are gradually weakened as the speed increases.

The experimental work-piece was fixed by means of spot welding, and the starting point of welding the assembly was set as the origin of the XYZ coordinate system. The coordinates of the edges of corrugated sheet along the y-axis and z-axis and upon surface of the base plate along the z-axis were obtained for curve fitting. The coordinates of each inflection point of the edge of the corrugated sheet and the corresponding point on the base plate were measured by the contact method based on the coordinate measuring machine. The graphical relationships obtained are shown in Figure 8-a, 8-b. For simplicity, only the data of the first ripple cycle is listed. The difference between the z- coordinate of a point on the edge of corrugated

sheet and the z-coordinate of the corresponding point on the base plate obtained by the contact method is the seam width of AG-W at that point. On this basis the seam width of AG-W along the length of the seam was obtained, and is shown in Figure 8-c. By calculating the values of half of seam width at each point, the trajectory of the centerline of AG-W was obtained, and is shown in Figures 8-a and 8-b.

In the tracking and monitoring of fillet welding of the corrugated sheet, Bi and Quan [15] used morphological operation to process the image and extract the feature points. In the experimental process, the seam width variation of AG-W obtained through dynamic monitoring at speeds of 0.3m/min, 0.6m/min, and 1.2m/min are shown in Figure 8-c. The variations of the centerline of AG-W obtained by dynamic monitoring along y-axis, z-axis at speeds of 0.3m/min, 0.6m/min, and 1.2m/min are shown as in Figures 8-a and 8-b.

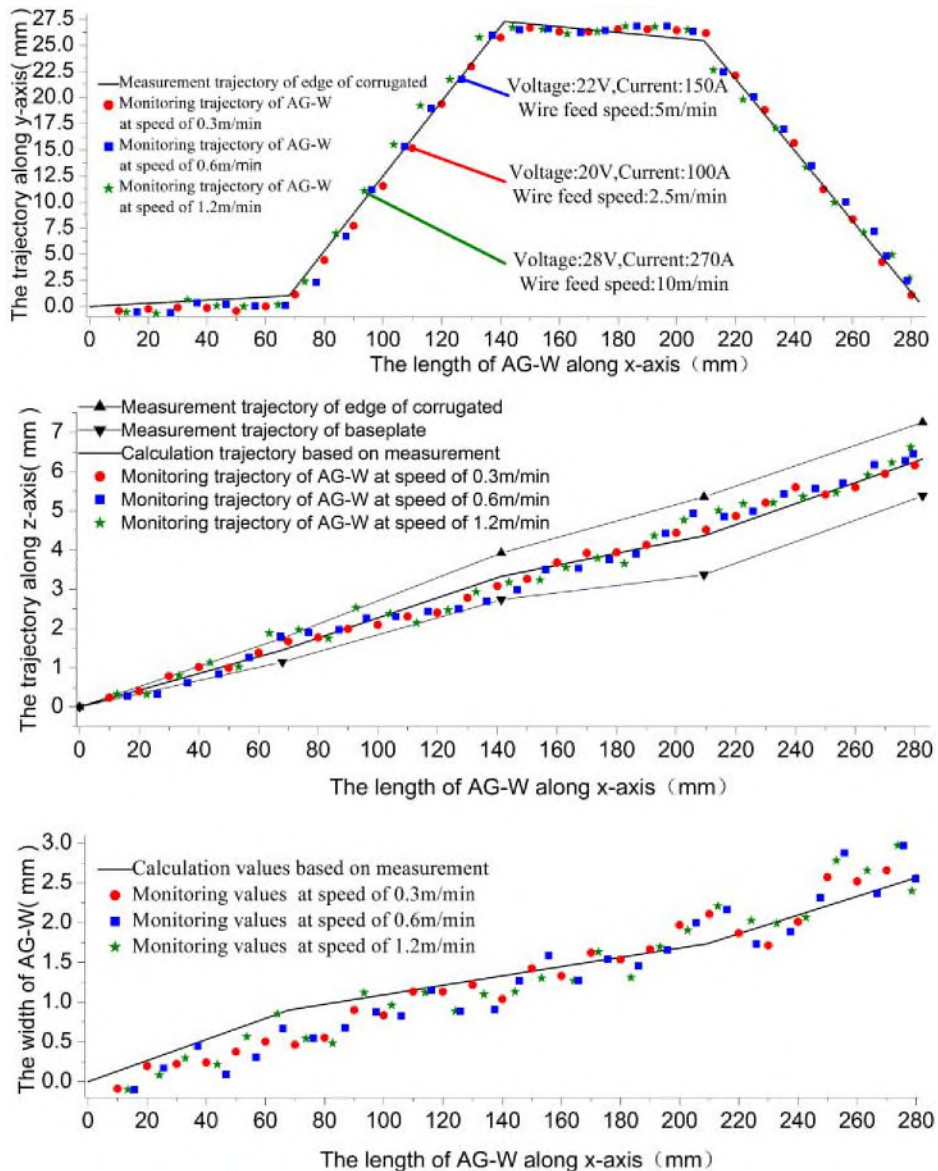


Figure 8. The Gap Width of AG-W and Trajectory of the AG-W: (a) The Trajectory of AG-W along the y-axis, (b) The Trajectory of AG-W along the z-axis, (c) The Gap Width of AG-W

On the basis of results presented in Figure 8, the following conclusions can be drawn.

(1) The monitoring error is largest at the corner. The main reason causing this error is the distortion of the projected periphery of small round corner;

(2) With increasing speed of the moving object, the monitoring accuracy slightly decreased. The main reason for the changes in accuracy is decreasing image quality.

(3) The accuracies of acquired seam width and centerline of 3-D trajectory of AG-W based on the single laser projection reach $\pm 0.5\text{mm}$. According to the deviation permissible in fillet weld as specified by GB50205-2001 and the research studies of Huang *et al.* [16], this accuracy satisfies the demand of high quality welding of container corrugated sheet.

(4) The main reason for the error to occur is due to the problem associated with the motion of two-dimensional platform and image calibration.

6. Conclusions

A visual and intelligent monitoring method and apparatus are theoretically analyzed and experimentally researched for the automatic fillet welding of corrugated sheet of a large structure. From the results of investigations through a series of welding experiments on the proposed system and with its algorithms, following are the conclusions:

(1) The visual tracking system of AG-W based on a single laser line is assembled and successfully tested.

(2) The geometrical relationships between image features, width and trajectory of AG-W are analyzed, and a mathematical model to describe the transformation between them is formulated.

(3) Under the optimized conditions, the reflected light is suppressed, and clear images of laser projection lines are obtained.

(4) The monitoring and tracking of the width and 3D trajectory of the assembly gap to be welded is achieved by combining online image acquisition, mathematical model and calibration parameters.

(5) By comparing the results obtained from this method with those of contacting method, it is found that the tracking of the seam width and trajectory of AG-W in the welding process reached an accuracy of $\pm 0.5\text{mm}$ or even better. This degree of error satisfies the demands of high quality welding, adjusting the welding parameters and guiding the motion trajectory of the torch of automatic welding system for container corrugated sheet.

Acknowledgements

The authors gratefully acknowledge the financial support received from the key project of the strategic cooperation between Guangdong Province and Chinese Academy of Science, 2013 (to be issued soon).

References

- [1] C. Y. Wu, P. C. Tung and C. C. Fu, "Development of an automatic arc welding system using an adaptive sliding mode control", *Journal of Intelligent Manufacturing*, vol. 21, (2010), p. 355-362.
- [2] S. Chokkalingham, N. Chandrasekhar and M. Vasudevan, "Predicting the depth of penetration and weld bead width from the infrared thermal image of the weld pool using artificial neural network modeling", *Journal of Intelligent Manufacturing*, vol. 23, (2012), pp. 1995-2001.
- [3] J. Y. Yu and S. J. Na, "A study on vision sensors for seam tracking of height-varying weldment", part 1: mathematical model. *Mechatronics*, vol. 7, (1997), pp. 599-612.
- [4] H. Luo and X. Chen, "Laser visual sensing for seam tracking in robotic arc welding of titanium alloys," *International Journal of Advanced Manufacturing Technology*, vol. 26, (2005), pp. 1012-1017.
- [5] M. Y. Kim, K. W. Ko, H. S. Cho and K. H. Kim, "Visual sensing and recognition of welding environment for intelligent shipyard welding robots", *Intelligent Robots and Systems* vol. 3, (2000), pp. 2159-2165.

- [6] D. X. Qiao, J. Zheng and J. L. Pan, "Dual structure laser vision sensor and its character", *Electric Welding Machine*, (Chinese), vol. 40, (2010), pp. 14-16.
- [7] M. S. Wu, M. L. Li and Z. F. Wu, "Study of a opto-mechanical scan system in three dimensions for multipurpose", *Journal of Tsinghua University (Sci & Tech)* vol. 37, (1997), pp. 29-31.
- [8] P. Q. Xu, X. H. Tan and S. Yao, "Application of circular laser vision sensor (CLVS) on welded seam tracking", *Journal Of Materials Processing Technology*, vol. 205, (2008), pp. 404-410.
- [9] J. B. Lu, "Weld seam detecting system based on circular scanning laser sensor", Dissertation, University of Shanghai Jiao Tong University, (Chinese), (2012).
- [10] Y. Huang, Y. L. Xiao, P. J. Wang and M. Z. Li, "A seam-tracking laser welding platform with 3D and 2D visual information fusion vision sensor system", *International Journal of Advanced Manufacturing Technology*, vol. 67, (2013), pp. 415-426.
- [11] X. C. Tian, G. X. Zhang and T. Liu, "Based on Laser Ranging corrugated containers welded track detection and control system", Patent, 200910015342.X (2009) (Chinese).
- [12] Q. L. Bi and Y. M. Quan, "Ripple Line Fillet Seam Tracking with Visual Sensors in Welding Process", *Key Engineering Materials*, (2014), pp. 46-51.
- [13] www.meta-mvs.com
- [14] D. H. Xie and Y. M. Quan, "Projector calibration method for structured light seam vision inspection system", *Electric Welding Machine*, (Chinese), vol. 43, (2013), pp. 46-51.
- [15] Q. L. Bi and Y. M. Quan, "Weld parameters information access based on laser line projected image", 2014 2nd Asian Pacific Conference on Mechatronics and Control Engineering (In Publishing) (2014).
- [16] W. Huang and R. Kovacevic, "Development of a real-time laser-based machine vision system to monitor and control welding processes", *The International Journal of Advanced Manufacturing Technology*, vol. 63, (2012), pp. 235-248.

Authors



Yanming Quan, She was born in 1957, is currently a professor in South China University of Technology, Guangzhou, China. His research interests include information system, measurement and control technology.



Qilin Bi, He was born in 1983. He is currently pursuing doctor degree at School of Mechanical & Automotive Engineering in South China University of Technology. His research interests include information system, measurement and control technology.